AIP Journal of Applied Physics

Dark current and trailing-edge suppression in ultrafast photoconductive switches and terahertz spiral antennas fabricated on multienergy arsenic-ion-implanted GaAs

Tze-An Liu, Gong-Ru Lin, Yen-Chi Lee, Shing-Chung Wang, Masahiko Tani, Hsiao-Hua Wu, and Ci-Ling Pan

Citation: Journal of Applied Physics **98**, 013711 (2005); doi: 10.1063/1.1953867
View online: http://dx.doi.org/10.1063/1.1953867
View Table of Contents: http://scitation.aip.org/content/aip/journal/jap/98/1?ver=pdfcov
Published by the AIP Publishing

Articles you may be interested in
Terahertz photomixing in high energy oxygen- and nitrogen-ion-implanted GaAs
Appl. Phys. Lett. **91**, 031107 (2007); 10.1063/1.2753738

Terahertz emission properties of arsenic and oxygen ion-implanted GaAs based photoconductive pulsed sources
J. Vac. Sci. Technol. A **24**, 774 (2006); 10.1116/1.2183284

Generation of continuous-wave terahertz radiation using a two-mode titanium sapphire laser containing an intracavity Fabry–Perot etalon
J. Appl. Phys. **97**, 103108 (2005); 10.1063/1.1904724

Fe-implanted InGaAs photoconductive terahertz detectors triggered by 1.56 m femtosecond optical pulses
Appl. Phys. Lett. **86**, 163504 (2005); 10.1063/1.1901817

THz radiation emission properties of multienergy arsenic-ion-implanted GaAs and semi-insulating GaAs based photoconductive antennas
J. Appl. Phys. **93**, 2996 (2003); 10.1063/1.1541105

Re-register for Table of Content Alerts

Create a profile.

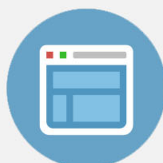

Sign up today!

[This article is copyrighted as indicated in the article. Reuse of AIP content is subject to the terms at: http://scitation.aip.org/termsconditions. Downloaded to] IP: 140.113.38.11 On: Thu, 01 May 2014 02:57:46

HTML ABSTRACT + LINKS

JOURNAL OF APPLIED PHYSICS 98, 013711 (2005)

Dark current and trailing-edge suppression in ultrafast photoconductive switches and terahertz spiral antennas fabricated on multienergy arsenic-ion-implanted GaAs

Tze-An Liu, Gong-Ru Lin,[a] Yen-Chi Lee, and Shing-Chung Wang
Department of Photonics and Institute of Electro-Optical Engineering, National Chiao Tung University, 1001 Ta Hsueh Road, Hsinchu 30010, Taiwan, Republic of China

Masahiko Tani
Institute of Laser Engineering, Osaka University, 2-1 Yamadaoka, Suita, Osaka 565-0871, Japan

Hsiao-Hua Wu
Department of Physics, Tunghai University, Taichung, Taiwan 407, Republic of China

Ci-Ling Pan[b]
Department of Photonics and Institute of Electro-Optical Engineering, National Chiao Tung University, 1001 Ta Hsueh Road, Hsinchu 30010, Taiwan, Republic of China

(Received 17 November 2004; accepted 20 May 2005; published online 13 July 2005)

We report ultrafast (~2.7 ps, instrument limited) switching responses of a multienergy-implanted GaAs:As^+ photoconductive switches (PCSs) with suppressed trailing edge and reduced dark current. This material is highly resistive with dark current as low as 0.94 μA at a bias of 40 V. The carrier mobility of the former is ~590 cm^2/V s, resulting in a small-signal optical responsivity of ~2 mA/W. Pumped at 100 mW and biased at 80 V, the multienergy-implanted GaAs:As^+ PCS exhibits peak response (0.35 V) comparable to the best result of single-energy-implanted ones. The improvement on photoconductive response is crucial for the generation of shorter terahertz emission pulses from spiral antennas fabricated on multienergy-implanted GaAs:As^+ (0.8 ps) than single-energy-implanted GaAs (1.2 ps), with the central frequency blueshifted to 0.2 THz (from 0.15 THz) and the spectral bandwidth broadened to 0.18 THz (from 0.11 THz). © *2005 American Institute of Physics*. [DOI: 10.1063/1.1953867]

I. INTRODUCTION

Photoconductive switches (PCSs) with ultrashort photoexcited carrier lifetime, good optical responsivity, high breakdown field, and low dark current are essential for fabrication of optically triggered terahertz antennas.[1,2] To meet these demands, various classes of carrier-lifetime-shortened semiconductors synthesized by impurity doping, radiation damage, chemical-vapor deposition, and molecular-beam epitaxy (MBE) have been explored. In particular, a nonstoichiometric GaAs film grown by MBE at low substrate temperatures (referred here after as LT-GaAs) with subpicosecond carrier lifetime was extensively used.[3,4] The absolute epitaxial growth temperature as well as the properties of LT-GaAs, however, is difficult to control due partly to lack of a reliable temperature monitoring instrument at such a low temperature (~200 °C) in high vacuum. As a result, the characteristics of LT-GaAs layers could vary even though the other growth parameters remain unchanged. Ion implantation has recently emerged as the most cost-effective method for preparation of substrate material for ultrafast PCS.[5] Carrier lifetimes as short as 0.2 ps have been reported for proton-bombarded GaAs, oxygen-implanted silicon on sapphire, and arsenic-ion-implanted GaAs (GaAs:As^+).[6,7] GaAs:As^+, which exhibits structural properties almost identical to LT-GaAs, exhibits a precisely and reproducibly controlled arsenic excess density in the implantation layer. After appropriate annealing, the highly resistive electrical and ultrafast optoelectronic properties of both GaAs:As^+ and LT-GaAs have made them the best candidates for PCS fabrication. The subpicosecond carrier lifetimes and picosecond photoconductive responses of GaAs:As^+ and LT-GaAs PCS were comparable.[8–10] Recently, the GaAs:As^+ has also been employed to fabricate optically controlled antennas for terahertz-wave generation and reception.[11,12] However, the reduction of the persistent falling-tail response and the saturating response at high biased voltages of the PCS made on either LT-GaAs or GaAs:As^+ substrate is still the important issues to be solved. The long photoexcited carrier decay in these materials can be entirely eliminated using either buffered layer epitaxy or high ion-dose implantation.[13] On the other hand, we expect that a more uniform implantation profile in the PCS through a multienergy or multidosage recipe would also be helpful in suppression of the trailing edge of the terahertz pulse shape and enable a faster emission response of the GaAs:As^+ PCS-based terahertz antenna. Other potential advantages include the improved breakdown characteristics of GaAs:As^+, which could result in higher emission efficiency of the antenna under a larger bias field.[10] In this work, we report on trailing-edge suppression and dark-current reduction properties of a multienergy-implanted and furnace-annealed GaAs:As^+ PCS and terahertz antenna. The

[a]Electronic mail: grlin@faculty.nctu.edu.tw
[b]Electronic mail: clpan@faculty.nctu.edu.tw

 © 2005 American Institute of Physics

[This article is copyrighted as indicated in the article. Reuse of AIP content is subject to the terms at: http://scitation.aip.org/termsconditions. Downloaded to] IP: 140.113.38.11 On: Thu, 01 May 2014 02:57:46

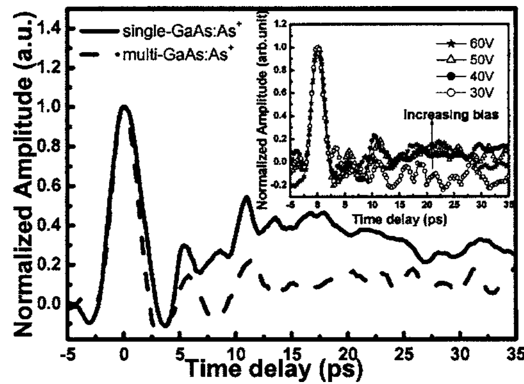

FIG. 1. Normalized photoconductive response and of single- (solid line) and multi- (dashed line) energy-implanted GaAs:As$^+$ PCSs at a bias voltage of 60 V as measured by the EOS technique. The inset shows the normalized photoconductive response of multienergy-implanted GaAs:As$^+$ PCS at different bias voltages.

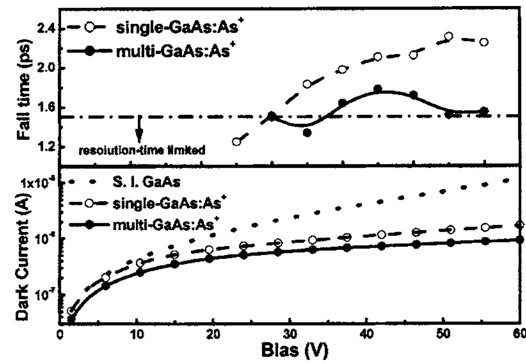

FIG. 2. Bias-dependent falling time (upper part) and dark current (lower part) of single- (circle dot) and multi- (square dot) energy-implanted GaAs:As$^+$ PCSs.

improvement on photoconductive response is crucial for the generation of shorter terahertz emission pulses from spiral antennas fabricated on multienergy-implanted GaAs:As$^+$ (0.8 ps) than single-energy-implanted GaAs (1.2 ps), with the central frequency blueshifted to 0.2 THz (from 0.15 THz) and the spectral bandwidth broadened to 0.18 THz (from 0.11 THz).

II. EXPERIMENT

The single-energy-implanted and multienergy-implanted GaAs:As$^+$ samples were prepared by first bombarding semi-insulating (SI) GaAs substrates with 200 KeV for the former and 50-, 100-, and 200-keV arsenic ions (As$^+$) for the latter, all at a dose of 10^{16} ions/cm^2. The samples were then furnace-annealing *ex-situ* at T_a=600 °C for 30 min. The choice of this annealing condition was based on good crystallinity, excellent dark resistivity, and ultrafast carrier lifetimes as determined by structural, electrical, and optical characterizations of the samples. The coplanar stripline (CPS) electrodes with 20-μm width and gap were fabricated on single- and multienergy-implanted GaAs:As$^+$ substrates. These devices were then characterized by an external electro-optic sampling (EOS) system with a homemade 60-μm-thick *X*-cut LiTaO$_3$ crystal as the electro-optic probe. The experimental setup of the EOS system was reported elsewhere.[9,10] It exhibits temporal and spatial resolutions of about 1 ps and 5 μm, respectively.

III. RESULTS AND DISCUSSIONS

The full-width-at-half-maximum (FWHM) responses of the single- and multienergy-implanted GaAs:As$^+$ PCS antennas are determined to be 3 and 2.7 ps, respectively (see Fig. 1). These correspond to 3-dB fast Fourier-transformed bandwidths of greater than 150 GHz. The bias dependence of the photoconductive responses of the multienergy-implanted GaAs:As$^+$ PCS is shown in the inset of Fig. 1. The switching speeds of both devices are similar, it is, however, worth noting that the trailing edges of the photoconductive responses of the multienergy-implanted GaAs:As$^+$ PCS are greatly suppressed. In multienergy-implanted GaAs:As$^+$ PCS with 60 V bias, the amplitude of the falling part is reduced to <15% of the peak response as compared to that of the single-energy-implanted GaAs:As$^+$ device (which still remains as high as nearly 50%). The fall time ($1/e$) of the single-energy-implanted GaAs:As$^+$ PCS slightly increases from 1.3 to 2.3 ps as the bias voltage increases from 25 to 60 V. By contrast, no apparent bias dependence of the falling time response was observed (~1.5 ps) for the multienergy-implanted GaAs:As$^+$ PCS (see the upper part of Fig. 2). The longer falling time of the single-energy-implanted GaAs:As$^+$ is attributed to the insufficient trapping of photoexcited carriers coming from bulk SI GaAs under high pumping density.[8] At higher bias, more photoexcited carriers in bulk SI GaAs with longer lifetime will also be collected, which inevitably increase the total response time of the single-energy-implanted GaAs:As$^+$ PCS. In contrast, the multienergy-implanted GaAs:As$^+$ has higher absorption coefficient and trapping center density, which not only helps limiting the penetration depth of photons but also enhances the trapping of photoexcited carriers from bulk SI GaAs. With the multienergy recipe, the necessity of an electric-buffer layer between the arsenic-rich layer and bulk GaAs is relaxed. The uniformity of arsenic antisite defects distributed in multienergy-implanted GaAs:As$^+$ is believed to contribute to the unchanged carrier trapping time as compared to single-energy-implanted GaAs:As$^+$.

The dark current of a multienergy-implanted GaAs:As$^+$ PCS antenna is relatively low as compared to those of single-energy-implanted and SI GaAs samples (see lower part of Fig. 2). The multienergy-implanted GaAs:As$^+$ PCS was found to be highly resistive with ultralow dark current of 0.94 μA at a bias of 40 V. This is about one-half that of the single-energy-implanted GaAs:As$^+$ PCS. At still lower bias, the dark current can be further reduced to 30 nA, which is far smaller than that of a PCS fabricated on a SI GaAs substrate.

The multienergy-implanted GaAs:As$^+$ exhibits uniformly distributed As precipitates and higher defect concentrations at a cost of degradation in carrier mobility as well as optical responsivity. As shown in Figs. 3(a) and 3(b), the optical responsivity of a multienergy-implanted GaAs:As$^+$ PCS at low pumping power is not as high as that of the single-energy-implanted GaAs:As$^+$ sample. Owing to the lower density and the larger effective mass of free carriers in

[This article is copyrighted as indicated in the article. Reuse of AIP content is subject to the terms at: http://scitation.aip.org/termsconditions. Downloaded to] IP: 140.113.38.11 On: Thu, 01 May 2014 02:57:46

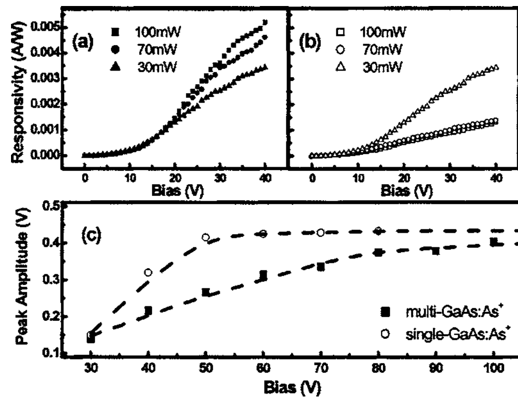

FIG. 3. Optical responsivity of (a) single- and (b) multienergy-implanted GaAs:As$^+$ PCS at pumping powers of 30 (triangular), 70 (circle), and 100 mW (square). (c) Peak amplitude of the transient photoconductive response from single- (circle dot) and multi- (square dot) energy-implanted GaAs:As$^+$ PCSs at different bias voltages.

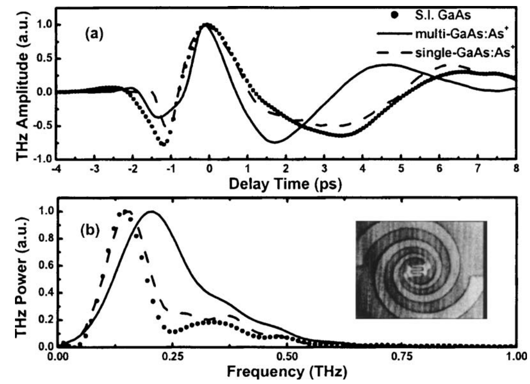

FIG. 4. The normalized terahertz radiation (a) wave forms and (b) power spectra from SI GaAs (circle dot), single- (dashed line) and multi- (solid line) dose GaAs:As$^+$ PCS-based spiral antennas.

multienergy-implanted GaAs:As$^+$, a much higher saturation power can be expected for the multienergy-implanted GaAs:As$^+$ PCS. In Fig. 3(c), we have plotted the peak amplitude of photoconductive responses of multi- and single-energy-implanted GaAs:As$^+$ PCSs as a function of bias voltage. Clearly, that of the multienergy-implanted GaAs:As$^+$ PCS exhibits a slower rising trend than the single-energy-implanted sample. Its magnitude, however, is eventually comparable to that of the single-energy-implanted device at a forward bias of >100 V. The optical responsivity of a multienergy-implanted GaAs:As$^+$ PCS at exciting power of 100 mW is 2 mA/W, which is slightly lower than that of a single-energy-implanted GaAs:As$^+$ PCS (5 mA/W). Nonetheless, these responsivities are better than ever reported for the LT-GaAs-based sample (1 mA/W).[8] At higher pumping powers (>100 mW), the photoconductive response of the single-energy-implanted sample at lower biases saturates (see Fig. 3). This can be explained by the intervalley carrier transfer (scattering of carriers from the Γ to L valley in the conduction band). In contrast, the response of a multienergy-implanted GaAs:As$^+$ PCS does not saturate until much higher bias ($\sim$90 V). The saturation fields are determined to be 25 and >45 kV/cm for single- and multienergy-implanted GaAs:As$^+$ samples, respectively. From these results, effective carrier mobilities for single- and multienergy-implanted GaAs:As$^+$ are estimated to be 1480 and 590 cm^2/V s, respectively, according to the following equation:[14]

$$I = e\mu\tau_c \frac{\eta\beta P(1-R)}{h\nu}\frac{V_{\text{bias}}}{d^2}, \quad (1)$$

where η is the quantum efficiency, β is the excitation efficiency, P is the average laser power, R is the reflectance coefficient, V_{bias} is the bias voltage, $h\nu$ is the photon energy of the laser, and d is the width of the photoconductive gap. The smaller carrier mobility in multienergy-implanted GaAs:As$^+$ infers that the effective mass of electrons in these materials could be much larger, since it is inversely proportional to the carrier mobility ($\mu \propto e\tau/\text{m}$).[15,16] The carrier trapping somewhat degrades the optical responsivity and effective carrier mobility of GaAs:As$^+$, however, it greatly improves the switching response.

To evaluate the terahertz emitting properties of these materials, planar photoconductive log-spiral antennas with metal-semiconductor-metal (MSM) interdigitated electrodes were patterned on the single- and multienergy-implanted GaAs:As$^+$ substrates. The finger width, area, and outer diameter of the 1.5-turn GaAs:As$^+$ PCS antennas are 5 μm, 35×35 μm^2, and 300 μm, respectively. Biased at 10 V and excited with 10 mW average power from a femtosecond mode-locked Ti:sapphire laser, the normalized terahertz radiation wave forms and frequency spectra detected using a LT-GaAs-based dipole antenna receiver[6] with probe power of 2.5 mW are shown in Figs. 4(a) and 4(b). The measured terahertz emission pulse widths of multi- and single-energy-implanted GaAs:As$^+$ antennas are 0.8 and 1.2 ps, respectively. The central frequencies (and spectral linewidths) of multi-energy-implanted GaAs:As$^+$ and single-energy-implanted GaAs:As$^+$ are 0.2 THz (0.18 THz) and 0.15 THz (0.11 THz), respectively. As a reference, those of a S.I. GaAs antenna were 0.14 THz (0.1 THz). The single-energy-implanted GaAs:As$^+$ antenna has a similar emission response to the SI GaAs one except a slightly shrunken falling tail of the terahertz pulse shape. The trapping of photoexcited carriers from bulk SI GaAs becomes more pronounced after multienergy implantation. Notably, the shorter emission time of the multienergy-implanted GaAs:As$^+$ antenna relies strongly on its fast photoconductive response. This extends the Fourier-transformed spectrum of the multienergy-implanted GaAs:As$^+$ antenna to a higher-frequency region.

IV. CONCLUSION

In conclusion, we report ultrafast ($\sim$2.7 ps, instrument limited) switching responses of a multienergy-implanted GaAs:As$^+$ photoconductive switches (PCSs) with suppressed trailing edge and reduced dark current. This material is highly resistive with dark current as low as 0.94 μA at a bias of 40 V, which is one-half that of single-energy-implanted GaAs:As$^+$. The carrier mobility of the former is, however, reduced to $\sim$590 cm^2/V s, resulting in a small-signal optical responsivity of $\sim$2 mA/W as compared to $\sim$5 mA/W of the latter. Nonetheless, the multienergy-

[This article is copyrighted as indicated in the article. Reuse of AIP content is subject to the terms at: http://scitation.aip.org/termsconditions. Downloaded to] IP: 140.113.38.11 On: Thu, 01 May 2014 02:57:46

implanted GaAs:As^+ PCS pumped at 100 mW and biased at 80 V exhibits peak response (0.35 V) comparable to the best result of single-energy-implanted ones. This is attributed to the higher breakdown threshold of the multienergy-implanted GaAs:As^+ PCS. The improvement on photoconductive response is crucial for the generation of shorter terahertz emission pulses from spiral antennas fabricated on multienergy-implanted GaAs:As^+ (0.8 ps) than single-energy-implanted GaAs (1.2 ps), with the central frequency blueshifted to 0.2 THz (from 0.15 THz) and the spectral bandwidth broadened to 0.18 THz (from 0.11 THz). The strong optical absorption and carrier trapping in the multidose-implanted GaAs:As^+ layer is essential for the shrinkage of the falling tail due to the effective suppression of residual carriers excited in bulk GaAs.

ACKNOWLEDGMENTS

This work was supported in part by the National Science Council of Taiwan under variant Grants and the Pursuit of Academic Excellence Program of the Ministry of Education of the ROC.

[1] N. M. Froberg, B. B. Hu, X. C. Zhang, and D. H. Auston, IEEE J. Quantum Electron. **28**, 2291 (1992).
[2] E. R. Brown, K. A. McIntosh, F. W. Smith, K. B. Nichols, M. J. Manfra, C. L. Dennis, and J. P. Mattia, Appl. Phys. Lett. **64**, 3311 (1994).
[3] A. C. Warren, N. Katzenellenbogen, D. Grischkowsky, J. M. Woodal, M. R. Melloch, and N. Otsuka, Appl. Phys. Lett. **58**, 1512 (1991).
[4] S. Gupta, M. Y. Frankel, J. A. Valdmanis, J. F. Whitaker, F. W. Smith, and A. R. Calawa, Appl. Phys. Lett. **59**, 3276 (1991).
[5] A. Claverie, F. Namavar, and Z. Liliental-Weber, Appl. Phys. Lett. **62**, 1271 (1993).
[6] F. Ganikhanov, G.-R. Lin, W. C. Chen, C. S. Chang, and C.-L. Pan, Appl. Phys. Lett. **67**, 3465 (1995).
[7] A. Krotkus, S. Marcinkevicius, J. Janski, M. Kaminska, H. H. Tan, and C. Jagadish, Appl. Phys. Lett. **66**, 3304 (1995).
[8] H. H. Wang, P. Grenier, J. F. Whitaker, H. Fujioka, J. Jasinski, and Z. Lilienthal-Weber, IEEE J. Sel. Top. Quantum Electron. **2**, 630 (1996).
[9] G.-R. Lin and C.-L. Pan, Appl. Phys. Lett. **71**, 2901 (1997).
[10] G.-R. Lin, W. C. Chen, S. C. Chao, C. S. Chang, K. H. Wu, T. M. Hsu, W. C. Lee, and C. L. Pan, IEEE J. Quantum Electron. **34**, 1740 (1998).
[11] T. A. Liu, M. Tani, and C.-L. Pan, J. Appl. Phys. **93**, 2996 (2003).
[12] T. A. Liu, M. Tani, M. Nakajima, M. Hangyo, and C.-L. Pan, Appl. Phys. Lett. **83**, 1322 (2003).
[13] M. Lambsdroff, J. Kuhl, J. Rosenzweig, A. Axmann, and J. Schneider, Appl. Phys. Lett. **58**, 1881 (1991).
[14] M. Tani, K. Sakai, and H. Mimura, Jpn. J. Appl. Phys., Part 2 **36**, L1175 (1997).
[15] S. Yngvesson, *Microwave Semiconductor Devices* (Kluwer Academic, Massachusetts, 1991), p. 9.
[16] A. Raymond, J. L. Robert, and C. Bernard, J. Phys. C **12**, 2289 (1979).

[This article is copyrighted as indicated in the article. Reuse of AIP content is subject to the terms at: http://scitation.aip.org/termsconditions. Downloaded to] IP: 140.113.38.11 On: Thu, 01 May 2014 02:57:46